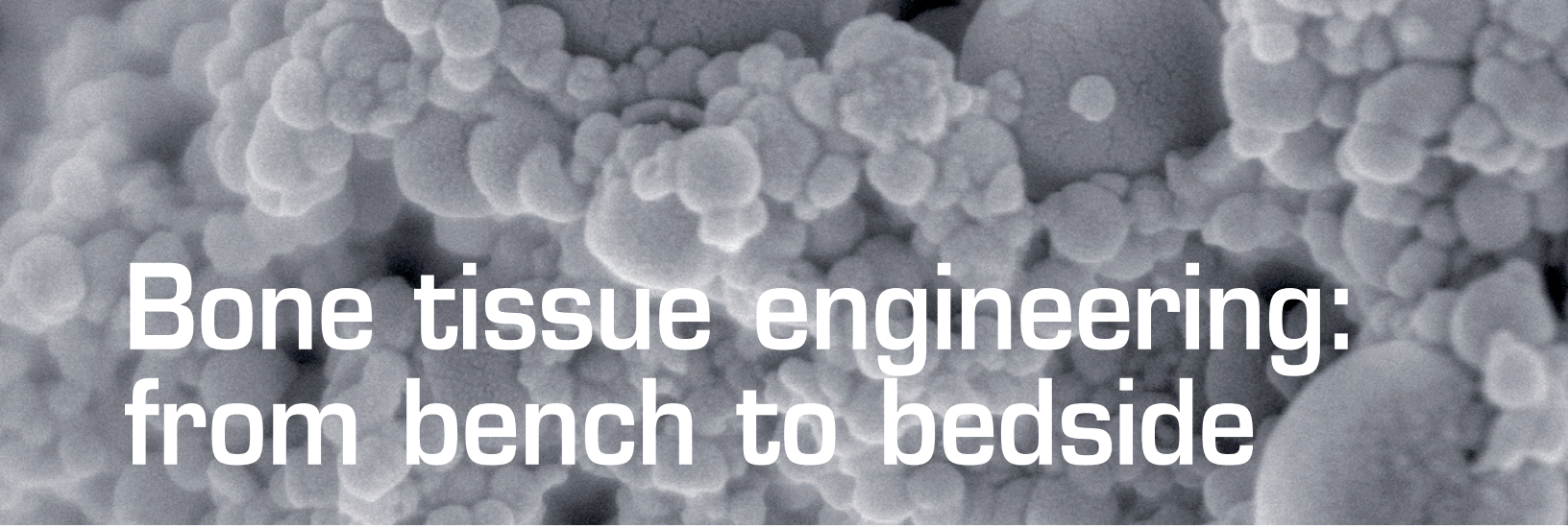

Bone tissue engineering: from bench to bedside

The drive to develop bone grafts for the filling of major gaps in the skeletal structure has led to a major research thrust towards developing biomaterials for bone engineering. Unfortunately, from a clinical perspective, the promise of bone tissue engineering which was so vibrant a decade ago has so far failed to deliver the anticipated results of becoming a routine therapeutic application in reconstructive surgery. Here we describe our bench to bedside concept, the first clinical results and a detailed analysis of long-term bone regeneration studies in preclinical animal models, exploiting methods of micro- and nano analysis of biodegradable composite scaffolds.

Maria A.Woodruff[a], Claudia Lange[b], Johannes Reichert[c], Arne Berner[d], Fulen Chen[e], Peter Fratzl[b], Jan-Thorsten Schantz[f], and Dietmar W. Hutmacher[a,g,h,*]
[a]*Institute for Health and Biomedical Innovation, Queensland University of Technology, 60 Musk Avenue, Kelvin Grove 4059, Australia*
[b]*Max Planck Institute of Colloids and Interfaces, Department of Biomaterials, Potsdam, Germany*
[c]*Department of Trauma, Hand, Plastic and Reconstructive Surgery, Julius-Maximillians-University, Wurzburg 97090, Germany*
[d]*IHBI and Department of Trauma Surgery, Univeristy of Regensburg, Regensburg 93053, Germany*
[e]*Departments of Oral and Maxillofacial Surgery, Fourth Military Medical University, Shaanxi, People's Republic of China*
[f]*Department of Plastic and Handsurgery, Klinikum rechts der Isar, Der Technischen Universität München, Germany*
[g]*Georgia Institute of Technology, Department of Mechanical Engineering, Atlanta, USA*
[h]*Institute for Advanced Study, Technische Universität München, Garching, Germany*
**E-mail: dietmar.hutmacher@qut.edu.au*

The field of tissue engineering is embodied in the collective vision of its early pioneers Langer and Vacanti, whose diverse yet symbiotic research approaches as an engineer and surgeon, led to the commencement of this interdisciplinary field. Their seminal 1993 paper remains one of the most influential and cited works in the field[1]. The application of the principles of biology and engineering to the development of functional substitutes for damaged tissue has seen laboratories worldwide forging impressive multi-disciplinary teams to focus on restoring, maintaining or improving the function of a wide range of human tissues[2-4]. While progress has been made to deliver bench to bedside solutions[5] (Fig. 1), the rate at which tissue engineering has seen innovations translated to the clinic has been slower than originally expected and the urgency for tissue-engineered products which achieve these ideals remains high[6-9].

Tissue engineered constructs (TEC)

The fundamental concept underlying tissue engineering is to combine a scaffold with living cells, and/or biologically active molecules to form a "tissue engineering construct" (TEC) which promotes the repair and/or regeneration of tissues[10,11]. The design of these scaffolds should consider physico-chemical properties, morphology and degradation kinetics. A suitable scaffold will (i) possess a porous interconnected pore network (pores & pore interconnections should be at least 400 microns to allow vascularization) with surface properties which are optimized for the attachment, migration, proliferation and differentiation of cell types of interest (depending on the targeted tissue) and enable flow transport of nutrients and metabolic waste, and (ii) be biocompatible and biodegradable with a controllable rate to compliment cell/tissue growth and maturation[12]. External size and

ISSN:1369 7021 © Elsevier Ltd 2012

shape of the construct are of importance, particularly if the construct is customized for an individual patient. Scaffold design and fabrication via additive manufacturing has advanced tremendously over the past few years[13]. The ability to create scaffolds in a layer by layer manner enables a computer aided design to be directly translated from a clinical scan (i.e., a patient CT scan) to produce customized scaffolds to fit an anatomical defect site[14-17].

Regeneration and remodeling of TECs

On implantation of a scaffold into a bone defect site, continuous cell and tissue remodeling is important for achieving stable biomechanical conditions and vascularization within the host site[18]. Importantly, TECs should stimulate and support both the onset and the continuance of bone in-growth as well as subsequent remodeling and maturation by providing optimal stiffness and external and internal geometrical shapes. Scaffolds must provide sufficient initial mechanical strength and stiffness to substitute for the loss of mechanical function of the diseased, damaged, or missing tissue and in addition must degrade at a rate which is compatible with new tissue in-growth and maturation[3,10]. This process is depicted schematically in Fig. 2, which illustrates the complex interplay of scaffold degradation with tissue formation and maturation. The scaffold is implanted at t = 0 (a,b) and over the first 7 days the scaffold becomes filled with a haematoma (c), followed by the formation of micro capillaries via angiogenesis. After 4 weeks, formation and invasion of larger blood vessels combined with the onset of bone formation can be detected within the scaffold (d). After 3 months, newly formed woven bone can be located throughout the scaffold architecture and the remodeling of the woven bone to lamellar bone takes place over a period of 6 to 12 month (e). The relationship over time between molecular weight loss-mechanical properties-physical weight loss and tissue regeneration is summarized in a graphical illustration (f). The mPCL-TCP scaffold starts degrading after 6 month via surface erosion and is completely resorbed after 3 years. The process is documented with SEM (g) and schematically illustrated (i).

It cannot be emphasized enough how essential it is to understand and control this scaffold degradation process, for successful tissue formation, remodeling, and maturation at the defect site. In the early days of tissue engineering, it was believed that scaffolds should degrade and vanish as the tissue is growing[19]. Yet, tissue in-growth and maturation differs temporally from tissue to tissue and, furthermore, tissue in-growth does not equate to tissue maturation and remodeling, in other words a defect filled with immature tissue should not be considered "regenerated". Hence, many scaffold-based strategies have failed in the past as the scaffold degradation was more rapid than tissue remodeling and/or maturation[20].

Translation of bone engineering concept from *bench to bedside*

Bone is accustomed to carrying major biomechanical loads, as a result nature has created bone to be a composite material, whose components are primarily collagen, non-collagenous proteins, and hydroxyapatite, yet whose complex structure contains a wealth of mechanically relevant details. Bone can be defined as a composite material in several senses, i.e., being a porous material, a polymer-ceramic mixture, a lamellar material and a fiber-matrix material. Its mechanical properties will therefore depend on each of these aspects of composition and structure. In general, bone displays a high intrinsic regenerative capacity following trauma or disease. Therefore, the majority of bone defects and fractures heal without any surgical intervention. Refinements in surgical techniques, implant design and postoperative care have significantly improved treatment outcomes of complex fractures and defects as caused by high energy trauma, disease, developmental deformity, revision surgery, and tumor resection[21-26]. Extensive soft tissue damage, insufficient surgical techniques, infections, and biomechanical instability can, however, lead to formation of large defects with limited intrinsic regenerative potential[27].

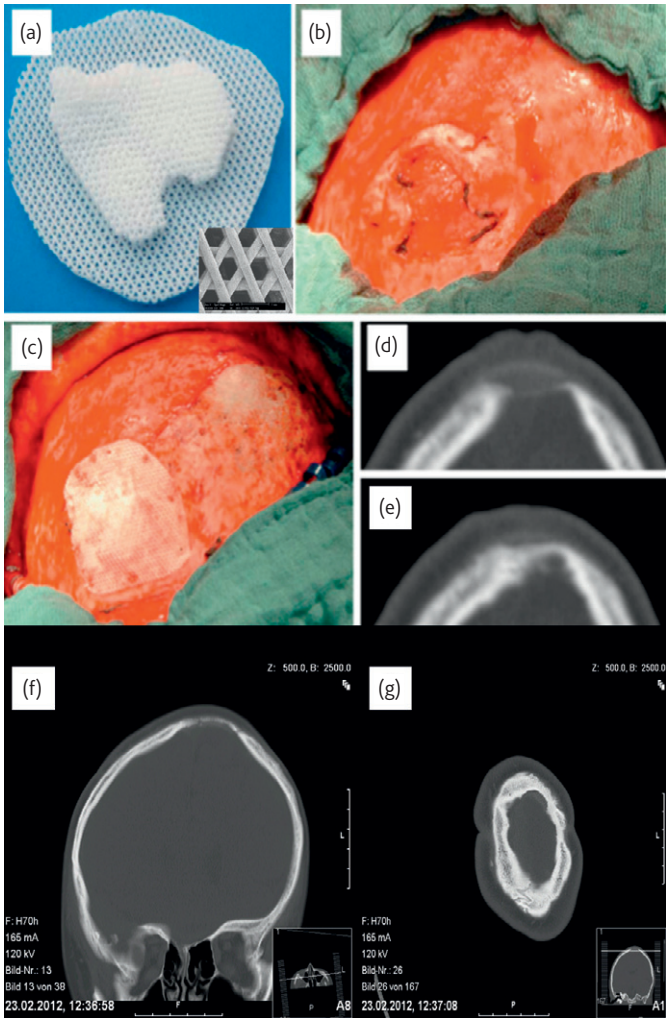

Fig. 1 The novel composite scaffold technology based on additive manufacturing developed at the National University of Singapore has been translated from bench to bedside. A medical-grade composite scaffold was designed based on medical CT imaging data and fabricated by fused deposition modeling (a), inset showing SEM of scaffold. A large calvarial defect (b) of a 9 year old girl was reconstructed with a custom-made and patient-specific composite scaffold (c). CT images (d, e, f, g) showing the defect before implantation of scaffold (d) and after 6 month implantation showing the beginning of consolidation of the defect (e) and complete filling of the scaffold architecture with bone after 24 months (f, g). Produced with permission from: Probst, F.A. et al., Handchir Mikroch P (2010) 42, 369.

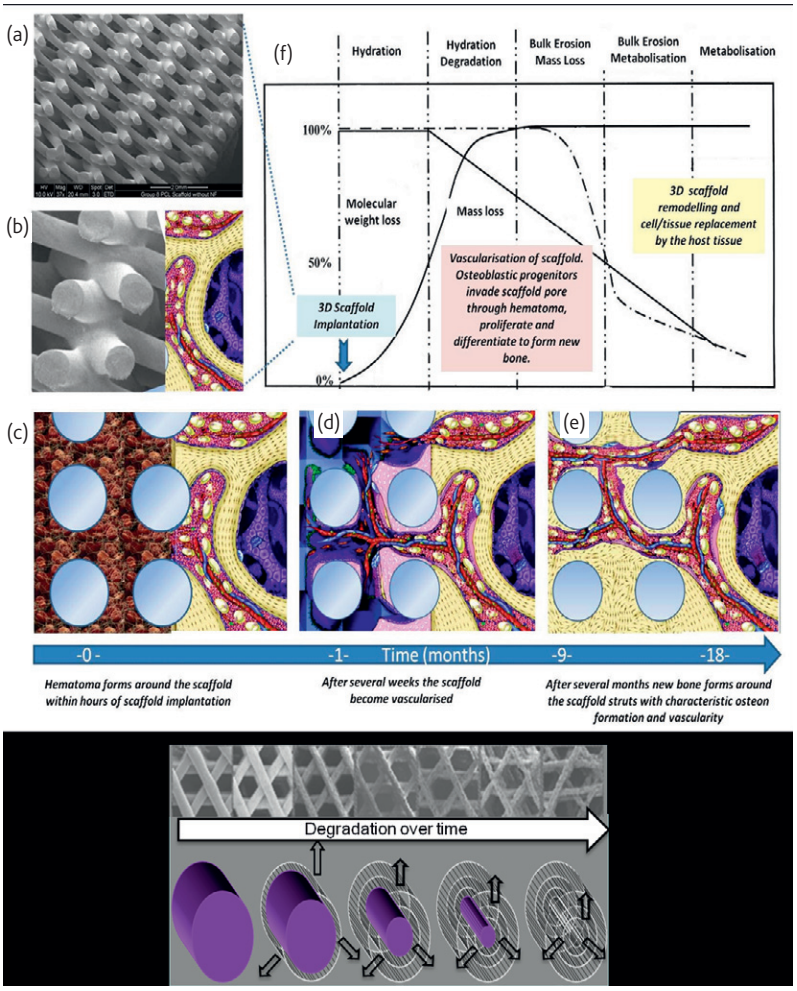

Fig. 2 Schematic illustrating the interdependence of molecular weight loss and mass loss of a slow-degrading composite scaffold plotted against time, which corresponds with tissue regeneration. Scaffold, as shown by SEM (a) is implanted at t = 0 (b) with lower figures (c-e) showing a conceptual illustration of the biological processes of bone formation over time. The scaffold is immediate filled with a hematoma on implantation (c) followed by vascularization (d) and gradually new bone is formed within the scaffold (e). As the scaffold degrades over time there is increased bone remodeling within the implant site until eventually the scaffold pores are entirely filled with functional bone and vascularity. Images (c-e) partially adapted from Muschler 200418. SEM of scaffold degraded over time (g) with associated schematic visualization of how mPCL-TCP scaffolds degrade via long-term bioerosion process, which takes up to 36 months in vivo (h)[29].

These defects represent a considerable surgical challenge, are associated with high socio-economical costs, and highly influence patients' quality of life, both private and professional.

The motivation for our research and the focus on translating bone engineering concepts from bench to bedside is rooted in the limitations in solving the increasing, and somewhat difficult, orthopedic, dental, and reconstructive surgery problems facing society, and the final clinical outcome for patients, may be approached from the perspective of the nature of the graft material with which the surgeon works. Current clinically-established therapeutic approaches focus on the implantation of autograft and allografts, metal devices, and ceramic-based implants to assist repair of bone defects; all with inherent disadvantages. These constraints have triggered a need for new therapeutic concepts to design and engineer unparalleled structural and functioning bone grafts to replace current treatments. It is within this context that the field of bone engineering has emerged, through the integration of engineering, life sciences, molecular and cell biology, stem cell biology, and surgery[28].

We have spent the last decade translating a concept of bone tissue engineering based on slow biodegradable composite scaffolds comprising medical grade polycaprolactone (mPCL) and calcium phosphates (hydroxyapatite (HA),tricalcium phosphate (TCP)), from the ***bench to the bedside***[29-38]. After a large series of ***in vitro*** experiments we consequently performed small animal studies using mice, rat and rabbit models which demonstrated the ability of composite scaffolds in combination with growth factors such as bone morphogenic protein (BMP) or cells to promote bone regeneration within ectopic sites or critical sized cranial defects (reviewed in detail by Woodruff & Hutmacher[3]).

Large animal models

When selecting a large preclinical animal model a number of factors

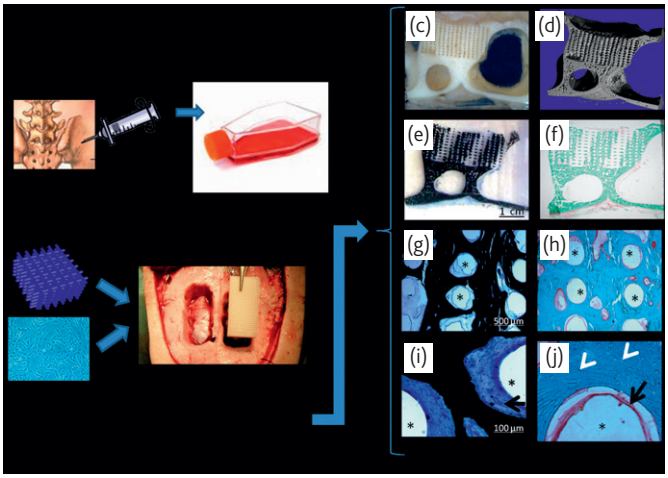

*Fig. 3 Schematic illustrating experimental set up and the bone regeneration process within mPCL-TCP scaffolds which were implanted within a critical sized porcine cranial defect for 2 years. BMSCs were extracted from the iliac crest and cultured for 2 weeks (a). mPCL-TCP scaffold containing 20 million BMSCs were implanted into critical sized cranial defects using fibrin glue as a cell carrier (b). After 2 years implantation the scaffolds and surrounding tissues were explanted (c), with the mPCL-TCP struts still clearly visible in the defect site with excellent integration. Samples were cut directly through the center before being analyzed using uCT (D) and sectioned at 6 µm for detailed histological analysis using von Kossa (e,g) and Goldner's trichrome staining (f,h) to reveal extensive bone formation within the scaffolds with almost 100 % of the pores filled with new bone (i,j). The scaffold struts (labeled *) dissolved during histological processing leaving clear evidence of surface erosion of the struts where new immature bone and osteoid (labeled with black arrows) has formed during the process of scaffold erosion (i,j). Osteoblasts are clearly seen active in the tissue surrounding the scaffold struts, with clear osteocytes embedded in mineralized matrix in the scaffold pores (labeled with white arrowheads).*

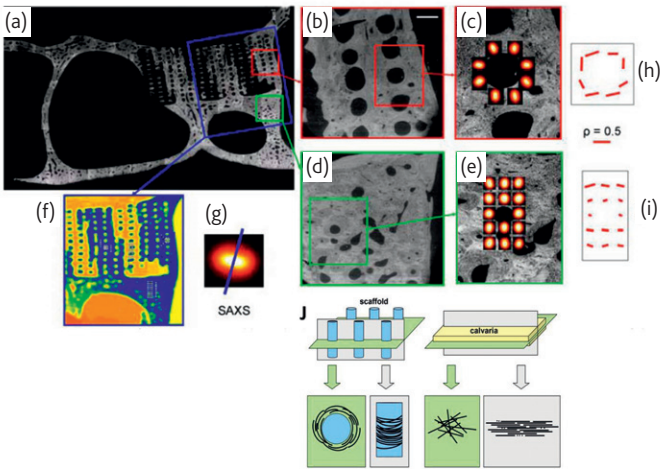

Fig. 4 Comparison of tissue engineered bone (red boxes) with normal bone (green boxes) in the vicinity of the implant. (a) Overview image, (b) and (c) enlargements of the ESEM pictures. The circles correspond to the location of struts in the implanted scaffold. Images (d) and (e) show enlargements of the ESEM pictures of normal areas next to the implant. (f) X-ray radiography image of the same specimen (blue areas correspond to high absorption). (g) Small-angle x-ray scattering (SAXS) patterns were collected at certain positions in the specimen. The asymmetry of the pattern is due to the alignment of the mineral particles in the volume illuminated by the x-ray beam. The blue line shows the typical orientation of the mineral platelets. (c) and (e) show SAXS patterns in the vicinity of an osteon (e) in normal bone or a scaffold strut (c) in tissue-engineered bone. The mean thickness of the mineral particles is 3.37 ± 0.16 nm near the osteon in (e) and 3.04 ± 0.25 nm near the scaffold strut in (c). (h, i) Typical orientation of the mineral particles as derived from the SAXS patterns in (c) and (e). It is clearly visible in (h) that the newly formed tissue is aligned parallel to the surface of the strut. A schematic drawing of the mineral arrangement in the tissue engineered bone and the calvaria, showing two different planes of view, is shown in (j). On the left, the scaffold architecture is schematically illustrated (top), with planes representing a top view in green and a side view in grey. The arrangement of the mineral particles is depicted for both planes (bottom). On the right, the calvarial plate and the mineral particle arrangement are schematically illustrated. The length of the bars in (h) and (i) corresponds to the degree of alignment ρ, as indicated. The bar in (b) corresponds to 200 microns.

need to be considered. The chosen model should clearly demonstrate close physiological and pathophysiological analogies with humans regarding the scientific question under investigation. Moreover, it must be manageable to operate and observe a multiplicity of study objects over a relatively short period of time[39-41]. Further selection criteria include costs for acquisition and care, animal availability, acceptability to society, tolerance to captivity and ease of housing[42].

Regeneration of a large bone skull defect

We have designed and executed a long-term, pre-clinical study (Fig. 3) to regenerate clinically relevant critical-sized cranial defects in pigs and have successfully demonstrated not only extensive bone regeneration but also remodeling over a period of two years within these defects treated with a mPCL-TCP scaffold with and without bone marrow derived mesenchymal stem cells (BMSC's). We used a suite of advanced analytical techniques to assess the properties of the tissue-engineered bone generated during these long-term *in vivo* studies, proposing that the onset of degradation should only occur after the regenerated tissue within the scaffold has remodeled at least once in the natural remodeling cycle. This paradigm shift is particularly relevant for higher load bearing tissues, such as bone. Original hypotheses in the field promoted scaffold degradation to onset immediately as new tissue starts to form. In contrast, we underline the importance of the scaffold remaining intact as the tissue matures in the scaffold pores with bulk degradation occurring later.

We demonstrate that this rationale, as depicted schematically in Fig. 2 leads to structural and functional bone regeneration in a large critical-sized skull defect model in pigs and show here a long-term bone engineering study which supports the theory of superior bone regeneration within slowly degrading composite scaffolds. Our post explantation analysis techniques enable bone quantity and quality to be assessed on the macro, micro and nano-scale. The comprehensive techniques presented here, which include microcomputed tomography, advanced mineralized hard-tissue resin histology, scanning electron microscopy and small angle x-ray scattering provides key insight into the cellular and extracellular matrix function and organization pertaining to long-term bone remodeling behavior within clinically relevant defect sites which are treated with a clinically proven tissue-engineered bone strategy (Fig. 3 and 4).

Scaffolds and the surrounding tissue were explanted after 2 years and it was observed that extensive bone regeneration had occurred within the defect sites containing mPCL-TCP scaffolds both with and without BMSC

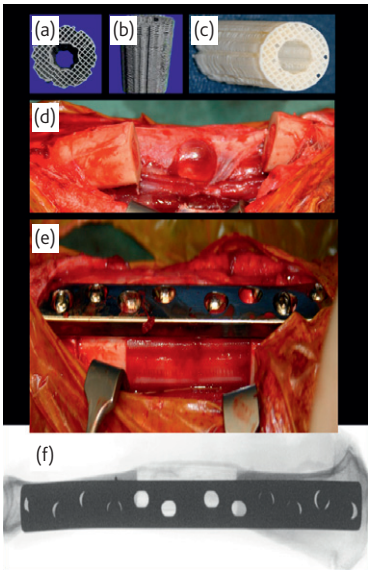

Fig. 5 A µCT image of the mPCL-TCP scaffold can be seen in (a) and (b) and a photograph of the scaffold at the implantation site are shown in (c, d). For the implantation of the composite scaffold loaded with 1 mg BMP-7 into a 6 cm segmental tibial bone defect, a skin incision was made over the medial part of the tibia. A dynamic compression plate (DCP) was positioned on the tibia and the screw holes are placed into the bone. The bone segment was removed after creating a 6 cm defect with an oscillating saw (D). Care was taken to completely remove the periosteum which is in the dorsal part very close to the vessels and the nerve. After the correct scaffold placement was tested the bone fragments were realigned and fixed with a DCP plate and screws. A medical grade biodegradable composite scaffold, mPCl-TCP, (diameter 18/6 mm, length 600 mm, 74 % fully interconnected porosity and pore size of 1 mm) loaded with 1 mg of BMP-7 was fitted into the defect and placed under compression by using the proximal screw holes of the DCP plate (e). Three month postoperative x-ray image shows the precise alignment of the proximal and distal tibia axes and the secure fixation of the DCP plate and scaffold and the bone formation across the scaffold architecture (f).

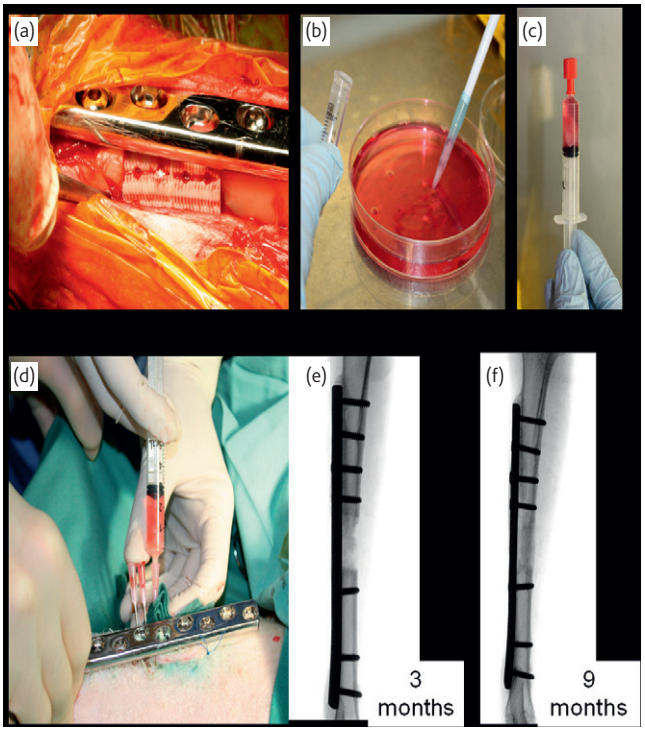

Fig. 6 In a recent study, we utilized delayed cell injection with cell matrix engineering that combines with composite scaffold technologies. Composite scaffolds were implanted into a 3 cm tibia defect (a) and allogenic BMSC were cultured under osteogenic conditions for 4 weeks to form a dense multiple layered cell sheet. The cell sheet was mechanically disrupted with a pipette (b) and the cells embedded in ECM were placed under sterile condition into a syringe (c). A fixation plate was used a guiding template (d) and the needles were placed minimally invasive into the scaffolds whilst injecting 200 million cells. The x-rays show that after 3 month post-injection there is evident bridging of the defect site (e) and the 9 month results show a very dense bone structure inside the composite scaffold (f).

addition. The scaffolds pores were filled with regenerated mineralized bone (Fig. 3 c-d) with extensive bone remodeling evident around scaffold struts and clear evidence of surface degradation of the composite scaffold matrix (Fig. 3g-j). The scaffold architecture was still evident within the defect sites after 2 years of implantation and the pores were seen to be completely filled with tissue, identified as mineralized bone (Fig. 3c-j).

Micro-computed tomography was performed to determine the bone volume fraction and bone mineral density and 3D rendered images were generated to demonstrate the extent of mineralization throughout the entire scaffold (Fig. 3d). Histological assessment (Fig. 3e-j) using von Kossa staining with Macneal's tetrachrome counter stain highlights the black mineralized tissue reflecting near complete mineralization within the scaffold pores (Fig. 3e,g,i). The slow process of surface erosion and degradation of the scaffold struts is also evident along with remodeling taking place within the pores (Fig. 3g-j). Goldner's trichrome staining (Fig. 3f,h,j) reveals striking osteocytes (white arrow heads) embedded within the mineralized matrix. There is notable osteoid formation around the scaffold struts (black arrows) demonstrating a tissue remodeling and maturation occurring as the scaffold gradually degrades via surface erosion enabling new bone to progressively replace the mPCL-TCP scaffold itself as it slowly erodes.

The calcium content of both the tissue-engineered bone and the native bone in adjoining regions of the skull was visualized by ESEM in backscattered electron mode (BSE) and small-angle x-ray scattering (SAXS) patterns were collected at certain positions in the specimen to ascertain mineral pattern alignment, as shown in Fig. 4, indicating that bone had been forming all around and in-between the scaffold struts (Fig. 4b,c). The areas corresponding to native calvarial bone show some porosity surrounded by bone material often with a lower mineral content (Fig. 4d,e). This indicated high remodeling activity, since lower mineral content usually means younger bone. Interestingly, the bone material surrounding the struts of the scaffold does not have a lower mineral density A possible explanation could be that the pores in the native calvaria gradually decrease by new bone formation at the inside of the pore, while tissue-engineered bone starts to grow on the surface of the struts and expands from there. As a consequence, the bone material around pore spaces in the skull is the youngest, while around the struts of the scaffold it is the oldest compared to the surroundings.

Regeneration of a large segmental tibial defect

Before translating new treatment concepts based on bone tissue engineering principles into a clinical application in orthopaedic and trauma surgery, rigorous evaluation in adequate preclinical animal models is absolutely essential. Several animal models have been developed over the years to verify the practicability of different research approaches in bone regeneration. Among these, adult sheep offer the advantage of having a comparable body weight, similar mineral composition of bone and similar metabolic and remodeling rates to patients and furthermore long bone dimensions suitable for the use of human fixation implants and prostheses, which is not possible in small animal studies. Thus, our group has established a challenging 3 cm[43] (Fig. 5) and 6 cm (Fig. 6) ovine segmental bone defect model using relatively old animals which possess the secondary osteon remodeling which is characteristic of human bone.

Our study results show that both a 3 cm[44] and a 6 cm critical-sized bone defect can be regenerated by recruitment and stimulation of endogenous cells by a scaffold which contains relevant growth factors. The bone regenerative potential of such a well-designed TEC, which contain a well characterized scaffold system with bone morphogenic proteins (BMPs; a family of growth factors which have been shown to stimulate growth, maturation and regulation of bone) has been shown by our group to outperform the current "gold standard": autograft after 12 month of implantation. This is substantiated by x-ray, clinical CT and micro CT scans, biomechanical, and histological assessment. Our work also shows that a composite scaffold loaded with 40 Mill. bone marrow-derived mesenchymal precursor cells stimulate more bone formation than the scaffold alone; however it shows significant lower bridging score and bone volume as the scaffold/BMP group. Hence, our current studies (Fig. 6) focus on increasing the cell implantation number and adapting scaffold design which allow the minimal invasive injection of cells 4 – 6 weeks after the implantation of the scaffold to overcome the initial inflammation period related to the surgery and defect creation and to inject the cells at the time of early vascularization of construct.

Summary and outlook

A well-engineered scaffold for bone tissue engineering which is suitable to be translated from the bench to the bedside combines inspired design, technical innovation and precise craftsmanship. Original thinking in the field endorsed scaffold degradation to occur as soon new tissue started to form. In contrast, we emphasize the importance of the scaffolds remaining intact as newly formed tissue matures within the porous and fully interconnected scaffold architecture and that the onset of degradation should only occur after the regenerated tissue has remodeled at least once in the natural remodeling cycle. The importance of long-term preclinical animal studies followed by in depth analysis of different orders of magnitude from macro- to micro to nano scale, using sophisticated methods to prove the outcome of highly organized and functional regenerated bone is crucial to future development and optimization of TECs. mt

References

1. Langer, R. and Vacanti, J. P., *Science* (1993) **260**, 920.
2. Scotton, C. J., *Materials Today* (2011) **14**, 212.
3. Woodruff, M. A. and Hutmacher, D. W., *Progress in Polymer Science* (2010) **35**, 1217.
4. Peck, M. *et al.*, *Materials Today* (2011) **14**, 218.
5. Probst, F. A. *et al.*, *Handchir Mikrochir P* (2010) **42**, 369.
6. Discher, D. E., Mooney, D. J., and Zandstra, P. W., *Science* (2009) **324**, 1673.
7. Grafahrend D. *et al.*, *Nat Mater* (2010) **10**, 67.
8. Griffith, L. G. and Naughton, G., *Science* (2002) **295**, 1009.
9. Service, R. F., *Science* (2005) **309**, 683.
10. Hutmacher, D. W., *Biomaterials* (2000) **21**, 2529.
11. Warnke, P. H. *et al.*, *Biomaterials* (2006) **27**, 3163.
12. Park, H. *et al.*, *Tissue Engineering* (2007) **13**, 1867.
13. Melchels, F. P. W. *et al.*, *Progress in Polymer Science* (2012) **37**, 1079.
14. Schantz, J. T. *et al.*, *J Mater Sci-Mater Med* (2005) **16**, 807.
15. Schantz, J. T. *et al. Mary Ann Liebert Inc Publ* (2003) **S127-S139**.
16. Schantz, J. T. *et al. Mary Ann Liebert Inc Publ* (2003) **S113-S126**.
17. Zein, I. *et al.*, *Biomaterials* (2002) **23**, 1169.
18. Muschler, G. E., Nakamoto, C. and Griffith, L. G., *J Bone Joint Surg-Am Vol* (2004) **86A**, 1541.
19. Khademhosseini, A., Vacanti, J. P. and Langer, R., *Scientific American* (2009) **300**, 64.
20. Moutos, F. T., Freed, L. E. and Guilak, F., *Nat Mater* (2007) **6**, 162.
21. Perka, C. *et al.*, *Biomaterials* (2000) **21**, 1145.
22. Komaki, H. *et al.*, *Biomaterials* (2006) **27**, 5118.
23. Gugala, Z. and Gogolewski, S., *Injury* (2002) **33** Suppl 2, B71.
24. den Boer, F. C. *et al.*, *J Orthop Res* (2003) **21**, 521.
25. Laurencin, C., Khan, Y. and El-Amin, S. F., *Expert Rev Med Devices* (2006) **3**, 49.
26. Wildemann, B. *et al.*, *Cell Tissue Bank* (2007) **8**, 107.
27. Perry, C. R., *Clinical orthopaedics and related research* (1999) **71**.
28. Berner, A. *et al.*, *Cells and Tissue Research* (2011).
29. Abbah, S. A. *et al.*, *Mary Ann Liebert Inc* (2008) **OP3.**
30. Christopher, X. F. L. *et al.*, *J Biomed Mater Res Part A* (2009) **90A**, 906.
31. Hutmacher, D. W. *et al.*, *J Tissue Eng Regen Med* (2007) **1**, 245.
32. Lam C. X. F. *et al.*, *Biomed Mater* (2008) **3**, 15.
33. Lam, C. X. F., Teoh, S. H., and Hutmacher, D. W., *Polym Int* (2007) **56**, 718.
34. Rai, B. *et al.*, *Biomaterials* (2004) **25**, 5499.
35. Rai, B., *et al.*, *Biomaterials* (2005) **26**, 3739.
36. Sawyer, A. A. *et al.*, *Biomaterials* (2009) **30**, 2479.
37. Zhou, Y. F. *et al.*, *Biomaterials* (2007) **28**, 814.
38. Zhou, Y. F. *et al.*, *Polym Int* (2007) **56**, 333.
39. Egermann, M., Goldhahn, J. and Schneider, E., *Osteoporos Int* (2005) **16** Suppl 2, S129.
40. Liebschner, M. A., *Biomaterials* (2004) **25**, 1697.
41. Schimandle, J. H. and Boden, S. D., *Spine* (1994) **19**, 1998.
42. Pearce, A. I., *et al. Eur Cell Mater* (2007) **13**, 1.
43. Reichert, J. C., *et al. Tissue Eng Part B Rev* (2010) **16**, 93.
44. Reichert, J. C., *et al. Sci Transl Med* (2012) **4**(141), 141.